

Functional interaction between TRPC1 channel and connexin-43 protein: a novel pathway underlying S1P action on skeletal myogenesis

Elisabetta Meacci · Francesca Bini · Chiara Sassoli ·
Maria Martinesi · Roberta Squecco · Flaminia Chellini ·
Sandra Zecchi-Orlandini · Fabio Francini · Lucia Formigli

Received: 19 February 2010 / Revised: 7 June 2010 / Accepted: 21 June 2010
© Springer Basel AG 2010

Abstract We recently demonstrated that skeletal muscle differentiation induced by sphingosine 1-phosphate (S1P) requires gap junctions and transient receptor potential canonical 1 (TRPC1) channels. Here, we searched for the signaling pathway linking the channel activity with Cx43 expression/function, investigating the involvement of the Ca²⁺-sensitive protease, *m*-calpain, and its targets in S1P-induced C2C12 myoblast differentiation. Gene silencing and pharmacological inhibition of TRPC1 significantly reduced Cx43 up-regulation and Cx43/cytoskeletal interaction elicited by S1P. TRPC1-dependent functions were also required for the transient increase of *m*-calpain activity/expression and the subsequent decrease of PKC α levels. Remarkably, Cx43 expression in S1P-treated myoblasts was reduced by *m*-calpain-siRNA and enhanced by pharmacological inhibition of classical PKCs, stressing the relevance for calpain/PKC α axis in Cx43 protein remodeling. The contribution of this pathway in myogenesis was

also investigated. In conclusion, these findings provide novel mechanisms by which S1P regulates myoblast differentiation and offer interesting therapeutic options to improve skeletal muscle regeneration.

Keywords Stretch-activated channels · Gap junctions · Myogenesis · Bioactive lipids · Calpain

Introduction

Sphingosine 1-phosphate (S1P) is a well-described bioactive lipid mediator involved in the regulation of many essential cellular processes, including cell growth and survival, regulation of cell migration, and differentiation [1]. Its role in skeletal muscle cell biology is beginning to be highlighted by recent data showing that the sphingolipid is able to promote satellite cell activation and proliferation [2, 3],

E. Meacci · F. Bini · M. Martinesi
Department of Biochemical Sciences,
University of Florence, Viale GB Morgagni 50,
50134 Florence, Italy
e-mail: elisabetta.meacci@unifi.it

F. Bini
e-mail: fbini@unifi.it

M. Martinesi
e-mail: mmartinesi@hotmail.it

C. Sassoli · F. Chellini · S. Zecchi-Orlandini · L. Formigli (✉)
Department of Anatomy, Histology, and Forensic Medicine,
University of Florence, Viale GB Morgagni 85,
50134 Florence, Italy
e-mail: formigli@unifi.it

C. Sassoli
e-mail: csassoli@unifi.it

F. Chellini
e-mail: f_chellini@hotmail.com

S. Zecchi-Orlandini
e-mail: zecchi@unifi.it

R. Squecco · F. Francini
Department of Physiological Sciences, University of Florence,
Viale GB Morgagni 48, 50134 Florence, Italy
e-mail: roberta.squecco@unifi.it

F. Francini
e-mail: fabio.francini@unifi.it

E. Meacci · F. Bini · C. Sassoli · R. Squecco ·
S. Zecchi-Orlandini · F. Francini · L. Formigli
Interuniversity Institute of Myology (IIM), Florence, Italy

regulate myogenic differentiation [4–6], and exert a trophic action on denervated muscle [7]. S1P actions on skeletal myoblast differentiation are strictly dependent on intracellular Ca^{2+} mobilization [6, 8, 9], actin cytoskeletal remodeling, and mechanosensitive stretch-activated cation channel (SAC) opening [10, 11]. The formation of stress fibers by S1P has been associated with plasma membrane stretching and, in turn, with SAC activation in C2C12 myoblasts [12, 13]. Several members of the transient receptor potential canonical (TRPC) ion channel family are recognized as promising candidates for SACs in different cell types [14], including sensory neurons [15], vascular smooth muscle [16], endothelial cells [17], and skeletal myoblasts [4]. Of interest, our recent findings support the involvement of TRPC1/SACs channels in skeletal myogenesis, based on the findings that TRPC1, the isoform mainly expressed in C2C12 cells [4], is sharply up-regulated by stimulation with S1P and, its down-regulation by specific siRNA is able to negatively interfere with SAC-mediated currents as well as with myoblast differentiation and fusion elicited by S1P [4, 9]. Moreover, evidence points to a role of TRPC1 in store-operated Ca^{2+} entry in skeletal muscle and in the regulation of myoblast migration and fusion [18, 19]. Interestingly, store-operated channels have been recently demonstrated to be targets of S1P [8, 9]. However, despite the identification of the molecular identity and functional roles of TRPC1 in skeletal myoblasts, little is known about how this channel and its interaction with signaling molecules function within the structural context of living cells to produce the coordinated cellular behaviours required for myoblast differentiation.

There is a substantial body of evidence showing that connexin (Cx)-containing gap junctions are involved in the coordination of numerous cell functions and differentiation processes during organogenesis, through the establishment of direct intercellular communications between neighboring cells [20–22]. Cx43 protein is the predominant connexin in skeletal muscle and its involvement in myogenesis and muscle regeneration have been well documented [6, 23–25]. We have demonstrated that expression levels of Cx43 are greatly enhanced by S1P in C2C12 skeletal myoblasts and provided the basis for considering the gap junctional protein as an intracellular target of the pro-myogenic action of the sphingolipid [6]. Of interest, Cx43 may also perform a gap junction independent function, acting as an adaptor protein through its interaction with F-actin and associated proteins, and establishing an organization center for intracellular signal transduction [6, 26, 27]. Like many other membrane proteins, Cx43 also exhibits a rapid turnover (half-life of few hours) controlled by a complex interplay of events involving the protein synthesis/degradation, plasma membrane association, and gap junction internalization.

In this context, our studies and others have shown that Ca^{2+} -dependent events regulate Cx43 expression in skeletal myoblasts [6] as well as its trafficking, assembly, gating, and turnover [21, 28, 29].

On the basis of all these observations, in the present study, we investigated the functional relationship between TRPC1 channels and Cx43 protein in C2C12 myoblasts induced to differentiate by S1P, and analyzed the underlying signaling pathway. In particular, we sought to define the role played by S1P-mediated TRPC1 activation on the expression and activity of *m*-calpain, a Ca^{2+} -sensitive protease, whose levels increase during early myogenic differentiation and after mechanical stimulation [30–33]. We also explored the functional repercussion of TRPC1-mediated *m*-calpain activation in the regulation of classical PKCs, Cx43 remodeling and myoblast differentiation and fusion.

Materials and methods

Cell cultures and treatments

Murine C2C12 skeletal myoblasts obtained from American Type Culture Collection (ATCC, Manassas, VA, USA) were cultured and induced to differentiate in differentiation medium (DM), DMEM (Invitrogen, Eugene, OR, USA) containing 2% horse serum (HS, Invitrogen) in the absence or presence of sphingosine 1-phosphate for 24–48–72 h (S1P, 1 μM ; stock 2 mM in 0.1% DMSO Calbiochem, San Diego, CA, USA), as previously reported [6]. Some experiments were performed pre-treating the cells with 50 μM gadolinium chloride (GdCl_3 , Sigma, Milan, Italy; stock 10 mM in 0.1 M HEPES pH 7.3, Sigma), a commonly used pharmacological blocker of SACs and SOCs [4, 34], with 30 μM carbobenzoxy-Val-Phe-CHO (MDL28170, stock 50 mM in 0.1% DMSO, Sigma) [35] and with 5 μM Gö6976 (stock in 0.1% DMSO, Tocris Bioscience, Bristol, United Kingdom), a selective inhibitor of classical PKCs. All the inhibitors were given 30 min prior to S1P stimulation.

Silencing of TRPC1 and *m*-calpain by siRNA

To inhibit the expression of TRPC1, a mix of short interfering RNA duplexes (siRNA) (Santa Cruz Biotechnology, Santa Cruz, CA, USA) corresponding to three distinct regions of the DNA sequence of mouse TRPC1 gene (NM_011643) as previously reported [4] was used. The expression of *m*-calpain was down-regulated using specific siRNA (Sigma) designed in two distinct regions of mouse *m*-calpain gene (NM_007600): 5' AGGUUGAUGAAGU GCUCUG 3'; 5' GAUCCUCUGCAAACCAAA 3'. A non-specific scrambled (SCR) siRNA was used as the

control. C2C12 myoblasts at 80% confluence were transfected using Lipofectamine 2000 reagent (1 mg/ml; Invitrogen) with TRPC1- or calpain-siRNA duplexes or with SCR-siRNA (20 nM) for 24 h, as previously reported [4, 5]. The specific knock-down of TRPC1 and *m*-calpain were evaluated by Western blotting or enzymatic assay or confocal immunofluorescence. The efficiency of transfection was estimated to range from 70 to 80%.

Confocal immunofluorescence

C2C12 cells grown on glass coverslips were processed for confocal microscopy examination as previously described [4]. Immunostaining was performed using the following primary antibodies: mouse monoclonal anti-connexin 43 (1:250; Chemicon, Temecula, CA, USA), rabbit polyclonal anti *m*-calpain (1:50; Sigma), rabbit polyclonal anti-TRPC1 (1:80; Santa Cruz Biotechnology) and mouse monoclonal anti-myogenin (1:50; Sigma). The immunoreactions were revealed by incubation with either goat anti-mouse Alexa 488-conjugated IgG (1:200; Molecular Probes Inc., Eugene, OR, USA), or goat anti-rabbit Alexa Fluor 488 or Alexa 568 conjugated IgG (1:200; Molecular Probes Inc.). Counterstaining was performed with tetramethylrhodamineisothiocyanate (TRITC)-labelled phalloidin (1:100; Sigma) to reveal F-actin filaments. In some experiments, living cells were first incubated with TRITC-conjugated wheat germ agglutinin (TRITC-WGA, 1:250; Molecular Probes Inc.) to label plasma membrane and then fixed and immunostained for calpain expression. The coverslips containing the immunolabeled cells were then viewed under a confocal Leica TCS SP5 microscope (Leica Microsystems, Mannheim, Germany) equipped with a HeNe/Ar laser source for fluorescence measurements and with differential interference contrast (DIC) optics. The observations were performed using a Leica Plan Apo 63X/1.43NA oil immersion objective. A series of optical sections (1024 × 1024 pixels each; pixel size 204.3 nm) 0.4 μm in thickness were taken through the depth of the cells at intervals of 0.4 μm. Images were then projected onto a single 'extended focus' image. When needed, a single optical fluorescent section and DIC images were merged to view the precise distribution of the immunostaining. Co-localization between TRITC-phalloidin and Cx43 fluorescence signals was evaluated by performing the analysis of the fluorescent signal distribution (scatterplot analysis) using the Leica Application Suite Software. Co-localization between calpain and TRITC-WGA signals was evaluated by Image J software (NIH, Bethesda, MD, USA).

Western-blot analysis

Immunoblotting was performed using enhanced chemiluminescence (ECL; Amersham Pharmacia Biotech,

Uppsala, Sweden) as previously reported [6, 36]. Total cell lysates, or membrane fractions, obtained from the subcellular fractionation procedures [37, 38], were resuspended in Laemmli's sample buffer and subjected to sodium dodecyl sulfate polyacrylamide gel electrophoresis (SDS-PAGE). Proteins were transferred on PVDF membranes (Hybond™-P, Amersham Pharmacia Biotech). To immunodetect endogenous proteins, specific rabbit polyclonal anti-TRPC1 (Santa Cruz Biotechnology), rabbit monoclonal anti-C-terminal region of connexin-43 (C6219; Sigma), mouse monoclonal anti-PKCα (Santa Cruz Biotechnology), rabbit polyclonal anti-cortactin (Sigma), and goat polyclonal anti-β-actin (Santa Cruz Biotechnology) antibodies were used. As loading control, the expression of β-actin was evaluated.

Immunoprecipitation

Immunoprecipitation was performed as previously reported [6, 38]. Briefly, cell lysates were resuspended in lysis buffer and, after pre-clearing with Protein A-Sepharose (Amersham Pharmacia Biotech), 2 μg of primary antibody (anti-Cx43) was added. Antibody-protein complexes were collected with Protein A-Sepharose. The immunocomplex was washed and dissolved in 4× Laemmli, proteins separated by SDS-PAGE and immunoblotted using anti-cortactin antibodies.

Electrophysiological measurements

Transmembrane ion current was measured in single C2C12 cells by whole-cell patch-clamp technique in voltage-clamp conditions, as previously described [4]. In these experiments, K⁺ and Na⁺ currents were suppressed using a TEA-Ca²⁺ bath solution containing (in mM) 2 CaCl₂, 145 TEABr and 10 HEPES, leaving Ca²⁺ as the only permeant cation. The patch pipettes were filled with solution containing (in mM) 150 CsBr, 5 MgCl₂, 10 EGTA, and 10 HEPES. The pH was titrated to 7.4 and to 7.2 with TEA-OH for bath and pipette solution, respectively. When filled, the resistance of the pipettes measured 1.3–1.7 MΩ.

SAC and/or SOC-mediated current (I_m) was determined by subtracting the leak current ($I_{m,leak}$) from the total current (I_m). The leak current was evaluated as the residual current recorded 3 min after adding the SAC/SOC blocker GdCl₃ (50 μM; Sigma) to the bath solution at the end of any experimental session. The SAC and/or SOC conductance (G_m) given in the results for any experimental conditions was evaluated from I_m .

The evaluation of intercellular currents through gap junctions was performed in C2C12 cell pairs by dual whole-cell patch-clamp, as previously described [6]. Briefly, the membrane potentials of *cell 1* (V_1) and *cell 2* (V_2) were

clamped to the same holding potential, $V_h = 0$ mV. V_1 was then changed to establish a transjunctional voltage (V_j), $V_j = V_2 - V_1$. To this end, *cell 1* was stepped using a bipolar pulse protocol beginning at $V_j = \pm 10$ mV and continuing up to ± 150 mV in 20-mV increments. Currents recorded from *cell 2* corresponded to $-I_j$. We determined the amplitudes of transjunctional current, I_j , at the beginning (instantaneous current, $I_{j,inst}$) and at the end of each pulse (steady state current, $I_{j,ss}$). From those values we calculated the related conductances $G_{j,inst}$ and $G_{j,ss}$. The $G_{j,ss}$ voltage dependence ($G_{j,ss} - V_j$ plot) was best fitted by the Boltzmann function: $G_{j,ss} = (G_{max} - G_{min}) / \{1 + \exp[A(V_j - V_0)]\} + G_{min}$, where G_{max} is the maximal $G_{j,ss}$ conductance and G_{min} is the residual conductance. G_{max} was calculated from 10 mV step. Temperature was set at 22°C.

Calpain activity

Calpain activity was measured in intact C2C12 cells by using the membrane-permeable fluorescent peptide substrate *N*-succinyl-leu-tyr-7-amido-4-methylcoumarin (Sue-LLVY-AMC, Sigma), as previously reported [39]. The non-fluorescent Sue-LLVY-AMC, after cleavage by calpains, emits strong fluorescence at a wavelength of 460–480 nm, which was monitored by using a Thermo Fluoroskan Ascent FL microplate fluorescence reader. One hundred thirty micromolar Suc-LLVY-AMC was added to C2C12 myoblasts in serum-free medium further buffered with 40 mM HEPES in 96-well culture plates. The dye-loaded cells were scanned for 10 min to ascertain fluorescence consistency, and also to allow the fluorescent probe to reach equilibrium. The increase of fluorescence was then recorded for 2 h at 30°C after addition of 10 μ M ionomycin. For data analysis, fluorescence intensity of each scan was normalized with initial fluorescent intensity (F0) and to total protein of each well.

Statistical analysis

In immunoblot experiments, densitometric analysis of the bands was performed using Imaging and Analysis Software by Bio-Rad (Quantity-One). Band intensity was reported as relative percentage (means \pm SEM), obtained by calculating the ratio of specific protein on β -actin intensity and normalizing to control, set as 100. Statistical significance was determined by Student's *t* test, with a value of $p < 0.05$ considered significant. In calpain assay experiments, data were analyzed by one-way ANOVA.

In the immunofluorescence experiments, densitometric analysis of the intensity of Cx43, TRPC1, calpain and WGA fluorescence was performed on digitized images of C2C12 cells using ImageJ software (NIH). Data were

Fig. 1 TRPC1/ Ca^{2+} is required for SIP-induced Cx43 expression in differentiating C2C12 myoblasts. **a** Confluent C2C12 myoblasts were cultured in differentiation medium (DM) in the absence (–SIP) or presence of 1 μ M SIP (+SIP) for 24 h. In parallel experiments the cells were treated with 50 μ M GdCl₃ or transfected with scrambled siRNA (SCR-siRNA) or TRPC1-siRNA. Whole-cell patch-clamp experiments were performed in single cells as indicated in “Materials and methods”. Transmembrane ion conductance and cell capacitance were recorded in TEA- Ca^{2+} bath solution. Data are mean \pm SEM of 10–14 different recordings. * $p < 0.05$ TRPC1-siRNA versus GdCl₃. § $p < 0.05$ and §§ $p < 0.01$ SIP stimulated versus unstimulated; +++ $p < 0.001$ GdCl₃ versus vehicle HEPES 0.1 M (control) and TRPC1-siRNA versus SCR-siRNA. **b** Confocal immunofluorescence images of C2C12 cells grown on glass coverslips in proliferation medium (basal) and DM in the indicated experimental conditions, fixed and immunostained for Cx43 expression (*green*). Counterstaining was performed with TRITC-phalloidin to reveal actin filaments (*red*). Note that Cx43 is transiently up-regulated during myogenesis and its levels are significantly increased by SIP stimulation and reduced in the presence of GdCl₃. In the histogram is reported the densitometric analyses of Cx43 fluorescent signal in the indicated experimental conditions. * $p < 0.05$ SIP versus basal. ° $p < 0.05$ SIP + GdCl₃ versus SIP. The images are representative of at least three separate experiments with similar results. **c** Western-blot analysis. Aliquots of proteins from cell lysates (15 μ g), obtained from cells treated as described in **a**, were separated by SDS-PAGE and Cx43 immunodetected with specific monoclonal antibodies. P0, P1, and P2 form band intensity relative to β -actin is reported in the graphic as relative expression. The relative percentage of band intensity to control (myoblasts cultured in DM for 24 h) set as 100 (mean \pm SEM) is shown. A blot representative of at least three independent experiments with analogous results is shown. Statistical significance respect to control * $p < 0.05$ and ** $p < 0.01$; § $p < 0.05$ SIP + GdCl₃ versus SIP

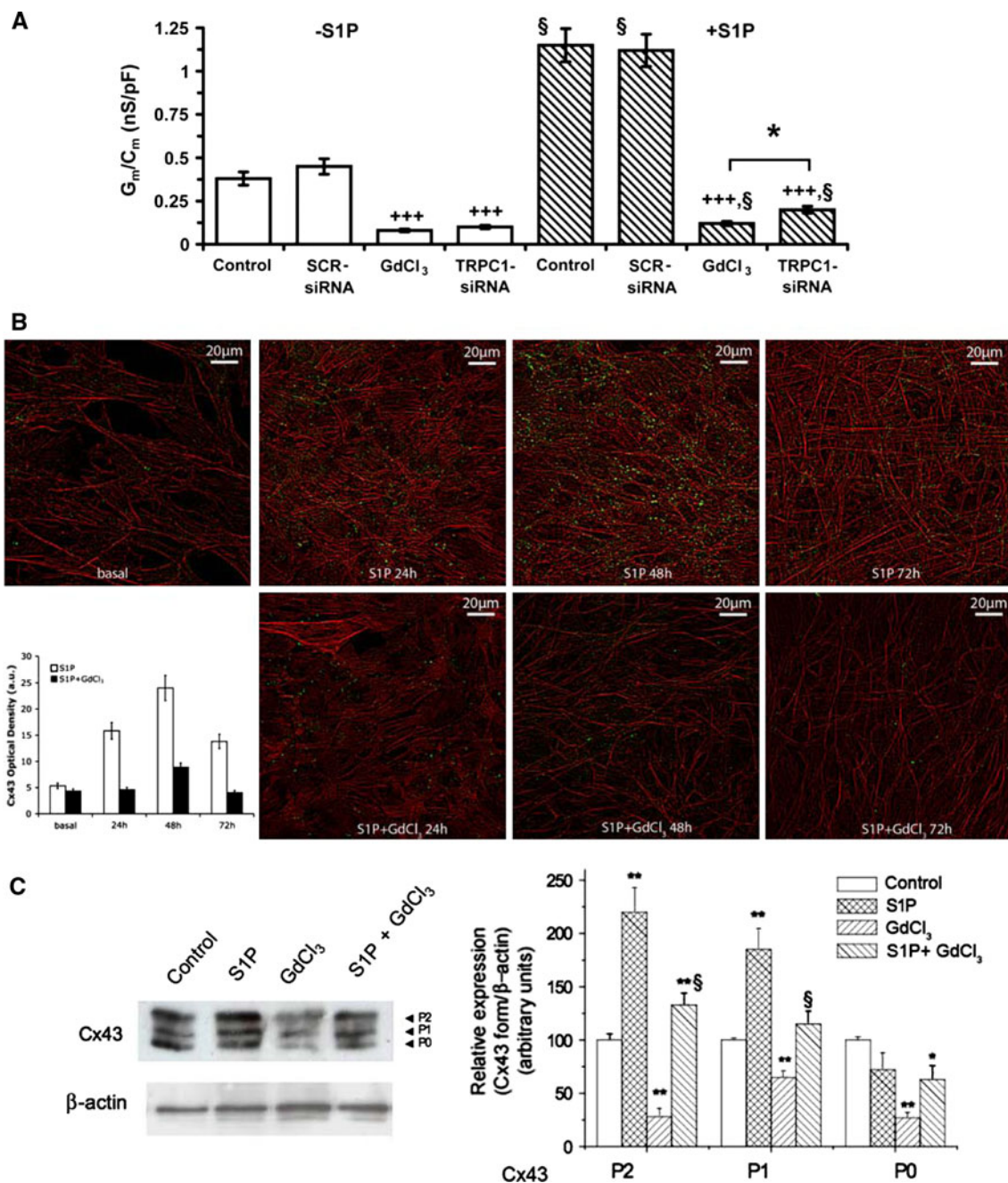
reported as a mean \pm SEM. At least 50 different cells were analyzed in each experiment (three preparations/experiment). Statistical significance was determined by using one-way ANOVA and a $p < 0.05$ was considered significant. Calculations were performed using GraphPad Prism software program (GraphPad, San Diego, CA, USA).

In electrophysiological experiments, statistical analysis of differences between the experimental groups was performed by one-way ANOVA and Newman–Keuls post-test ($p < 0.05$ was considered significant). Calculations were made with GraphPad Prism statistical program. pClamp9 (Axon Instruments, CA, USA), SigmaPlot and SigmaStat (Jandel Scientific, San Rafael, CA, USA) were used for mathematical and statistical analysis.

Results

TRPC1/ Ca^{2+} channels are involved in Cx43 expression/function in SIP-induced myoblast differentiation

To investigate the involvement of SAC/SOC channels in Ca^{2+} during the early phases of myogenesis, we performed patch-clamp analysis in differentiating C2C12 myoblasts in the presence or absence of specific channel inhibitors. The



results showed that when C2C12 cells were differentiated in the presence of S1P (1 μ M) for 24 h, the transmembrane Ca^{2+} current (G_m/C_m) significantly increased of approximately two folds as compared with those cultured in the absence of the bioactive lipid (Fig. 1a). This current was mainly dependent upon the activation of GdCl_3 -sensitive SAC/SOC channels. In fact, in unstimulated and S1P-stimulated cells, the treatment with 50 μ M GdCl_3 caused a 90% reduction in G_m/C_m as compared to the respective controls. Notably, TRPC1 channels were the

principal contributors to the recorded GdCl_3 -sensitive current in both unstimulated and stimulated cells, since G_m/C_m was reduced of approximately 75% in the cells where TRPC1 protein expression was specifically down-regulated by si-RNA (TRPC1-siRNA) (Fig. 1a). These data indicated the potential role of other channels in contributing to GdCl_3 -sensitive Ca^{2+} entry.

We next tried to explore whether the pro-myogenic action of S1P in these cells was related to the functional interaction between these Ca^{2+} channels and the gap

junction Cx43 protein. In agreement with our previous findings [6], confocal immunofluorescence showed that Cx43 protein was up-regulated by S1P (1 μ M) during the early stages of myogenesis, reaching the maximal expression at 48 h of differentiation (Fig. 1b). The treatment with 50 μ M GdCl₃ was able to prevent the transient increase of Cx43 in both the cytoplasm and along the peripheral stress fibers, in the regions compatible with the formation of gap junction plaques (Fig. 1b). By Western blotting, three bands of Cx43, with approximate molecular masses of 42, 44, and 46 kDa were immunodetected in C2C12 cell lysates: a fast-migrating form that includes the non-phosphorylated and phosphorylated forms (referred to as P0), and slow-migrating phosphorylated forms (termed P1 and P2) [21]. Stimulation with S1P increased Cx43 expression and affected its post translation modifications. The treatment with 50 μ M GdCl₃ attenuated the overall increase of Cx43 expression (P0 + P1 + P2) either in unstimulated and S1P-stimulated cells ($\cong 60$ and $\cong 50\%$, respectively), suggesting that SAC/SOC channel activation affected, although at different extent, the expression of both the nonphosphorylated and phosphorylated Cx43 isoforms. Silencing of TRPC1 also reduced the overall Cx43 protein expression ($\cong 60\%$ of control; $p < 0.05$, $n = 3$) (Fig. 2a, b). In particular, TRPC1-siRNA induced a robust decrease in the P0 and P1 forms, without substantially modifying the levels of P2 forms, which have been previously reported to correspond to Cx43 protein phosphorylated at specific serine residues (S325, S328, and/or S330) [40]. These data indicated that other GdCl₃-sensitive channels, rather than TRPC1, specifically regulated P2 forms.

Reduced Cx43 expression was associated with a significant impairment of the electrical gap junctional coupling, as measured by dual whole-cell voltage patch-clamp (Fig. 3). The treatment with 50 μ M GdCl₃ or transfection with TRPC1-siRNA, strongly reduced the amplitude of the transjunctional current (I_j) and steady-state conductance ($G_{j,ss}$) in unstimulated myoblasts and prevented the increase of these parameters in S1P-stimulated cells (Fig. 3A, B; Table 1). Notably, both the treatments (TRPC1-siRNA and GdCl₃) reduced, at a similar extent, the formation of homomeric connexons (i.e., connexons formed by one specific connexin isoform), as demonstrated by the shift of $G_{j,ss}$ at $+V_j$ towards more positive potentials as well as by the significant increase of the residual conductance (G_{min}) at $-V_j$ in the presence of S1P. The alterations in TRPC1 expression and function were also accompanied by a smooth dependence of $G_{j,ss}$ on negative voltage between the paired cells (Fig. 3C, Table 1), indicating an additional role of TRPC1 in the regulation of the channel selectivity. The greater $G_{j,ss}$

values and G_j symmetry of the Boltzmann curves observed in S1P-stimulated cells, further confirmed the role of S1P and TRPC1 in the regulation of gap junction electrical properties and the expression of homomeric connexons [6]. Taken together, all these results indicated that Ca²⁺ influx through TRPC1 was positively associated with Cx43 expression and intercellular coupling selectivity, suggesting, for the first time, a functional interaction between the two proteins in skeletal myoblast stimulated with S1P.

m-Calpain is regulated by S1P and TRPC1 channels and influences Cx43 expression and localization in differentiating myoblasts

We next investigated the involvement of TRPC1-mediated Ca²⁺ signaling elicited by S1P in the regulation of *m*-calpain, a Ca²⁺-dependent cysteine protease, previously shown to reach maximal activity at the beginning of the myogenic differentiation [33, 41].

We first showed that *m*-calpain was significantly enhanced within the first 48 h of C2C12 cell differentiation and this increase was potentiated by S1P (Fig. 4a). Transfection with TRPC1-siRNA or treatment with 50 μ M GdCl₃, prevented S1P-induced calpain activity, causing a decrease ($\cong 75\%$) in the protease activity, which was comparable to that promoted by specific *m*-calpain silencing (calpain-siRNA) or by treatment with 30 μ M MDL28170, a commonly used calpain inhibitor (Fig. 4b). Reduced TRPC1 activity also affected *m*-calpain expression and protein membrane association in S1P stimulated myoblasts (Fig. 4c–e), in agreement with the previously reported Ca²⁺-dependent expression and function of this protease in skeletal muscle [42]. Notably, the up-regulation of Cx43 induced by S1P also required *m*-calpain activation. Indeed, the treatment with MDL28170 as well as the specific silencing of *m*-calpain was able to significantly decrease (approximately 40%) the overall Cx43 expression (Fig. 5A–C) and its interaction with peripheral stress fibres at the plasma membrane (Fig. 5A). All these data provided intriguing evidence for an involvement of TRPC1-mediated Ca²⁺/*m*-calpain axis in the regulation of the expression/function of Cx43 levels in differentiating myoblasts and underscored a novel signaling pathway for the pro-myogenic action of S1P.

TRPC1/*m*-calpain/PKC α pathway affects Cx43 expression and cytoskeletal interaction in S1P-induced myoblast differentiation

It has been previously reported that PKC α is a good substrate for *m*-calpain [33]. We then explored the

involvement of this kinase in the regulation of Cx43 expression by TRPC1/calpain axis. According to previous findings [33], first we found a relationship between PKC α

and *m*-calpain activities during myogenic differentiation (Figs. 4a, 6); indeed, the pool of active membrane-associated PKC α decreased after the protease activation in

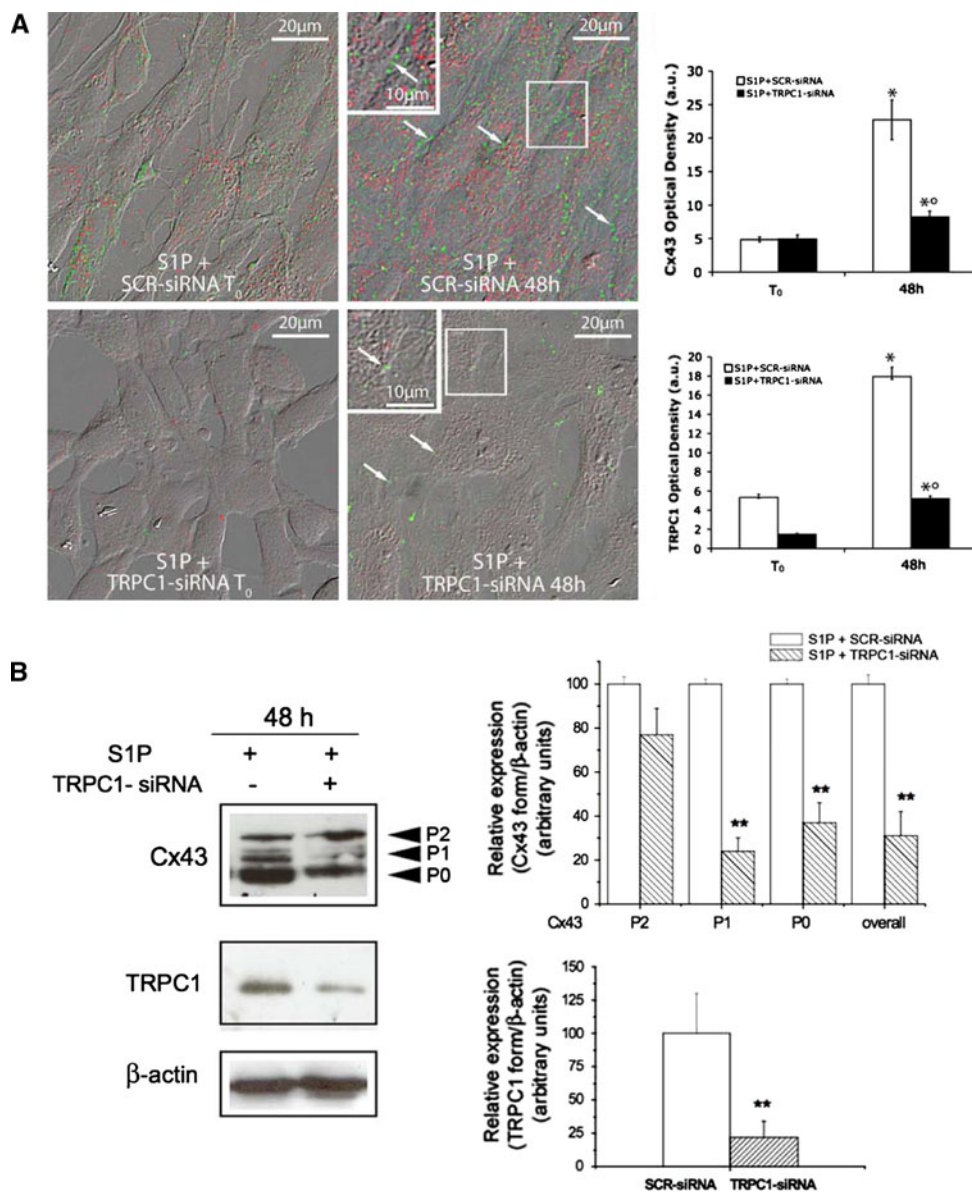


Fig. 2 TRPC1 silencing prevents S1P-induced Cx43 expression in differentiating C2C12 myoblasts. **a** C2C12 myoblasts were transfected with either scrambled siRNA (SCR-siRNA) or TRPC1-siRNA for 24 h. After 48 h from transfection (T₀) the cells were induced to differentiate by shifting in DM in the presence of 1 μ M S1P for 48 h. Superimposed DIC and confocal immunofluorescence images of S1P-stimulated C2C12 cells plated on glass coverslips fixed and immunostained with specific antibodies against TRPC1 (red) and Cx43 (green). Arrows indicate regions of cell-to-cell contacts. Insets. Magnifications of the outlined areas. Densitometric analyses of Cx43 and TRPC1 fluorescent signals are reported in the histograms. **p* < 0.05 S1P versus T₀, ^o*p* < 0.05 TRPC1-siRNA versus SCR-siRNA. The images are representative of at least three separate

experiments with similar results. **b** Western-blot analysis. Aliquots of proteins from lysates (20 μ g) obtained from cells transfected with SCR-siRNA (-) and TRPC1-siRNA (+) and incubated in DM in the presence of S1P (+) for 48 h, were separated by SDS-PAGE and Cx43 and TRPC1 expression analyzed using specific antibodies. P0, P1, and P2 form and the overall Cx43 band intensity relative to β -actin are reported in the graphic. Band intensity, reported as relative percentage to control, was arbitrarily normalized to 100. A blot representative of at least three independent experiments with similar results is shown. ***p* < 0.05 TRPC1-siRNA versus SCR-siRNA. Note the marked reduction of Cx43 signal in TRPC1-siRNA transfected cells compared to SCR-siRNA-treated ones at 48 h of differentiation

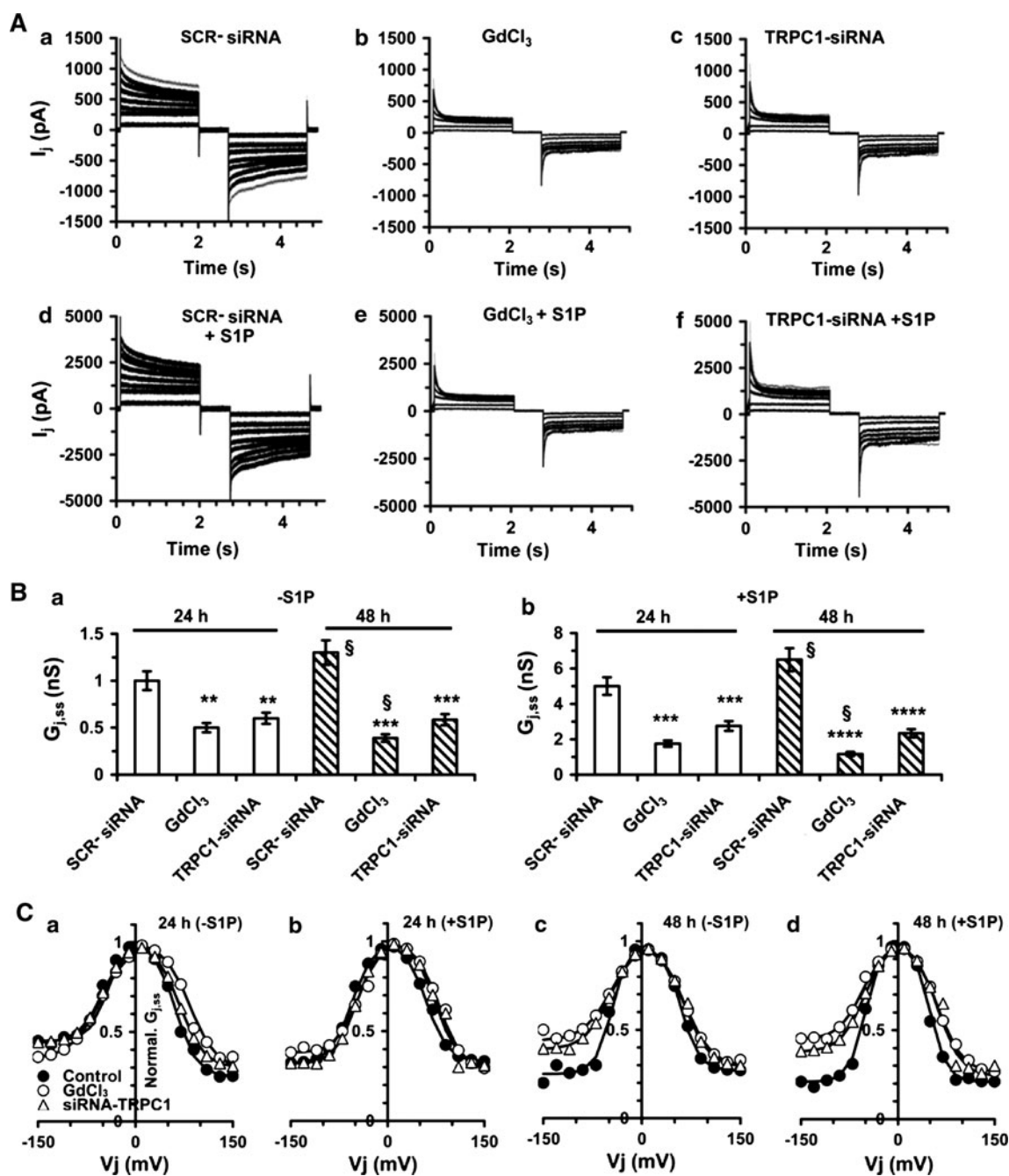


Fig. 3 Effects of S1P and inhibition of TRPC1 channels on gap-junctional electrical coupling of differentiating C2C12 myoblasts. **A** Representative time-course of transjunctional currents (I_j) recorded by dual patch-clamp in C2C12 myoblasts cultured in DM for 24 h in the indicated experimental conditions: **a, d** untreated or SCR-siRNA-treated cells, (SCR-siRNA); **b, e** 50 μ M $GdCl_3$ -treated cells; **c, f** TRPC1-siRNA-treated cells in the absence (**a–c**) and in the presence (**d–f**) of 1 μ M S1P (note the different ordinate scale in **d–f** respect to **a–c**). **B** Quantification of $G_{j,ss}$. Data are means \pm SEM normalized to SCR-siRNA at 24 h, as indicated in **A** in the absence

(**a**, $-S1P$) and in the presence (**b**, $+S1P$) of S1P. Data were evaluated at 24 and 48 h of differentiation. Data from vehicle or SCR-siRNA-treated cells (control) were not significantly different. $**p < 0.01$, $***p < 0.005$ and $****p < 0.001$ respect to SCR-siRNA at 24 h (**a**) and 48 h (**b**); $\S p < 0.05$ at 48 h respect to SCR-siRNA at 24 h. **C** Normalized $G_{j,ss}-V_j$ plots evaluated at 24 h (**a** and **b**) and 48 h (**c** and **d**) in the absence ($-S1P$) and in the presence ($+S1P$) of 1 μ M S1P in the same experimental conditions as reported in **A**. The absolute $G_{j,ss}$ values and Boltzmann parameters are shown in Table 1

Table 1 Boltzmann Parameters for gap Junctions in untreated and SCR-, GdCb-TRPC1- siRNA-treated C2C12 cell pairs stimulated or not with SIP

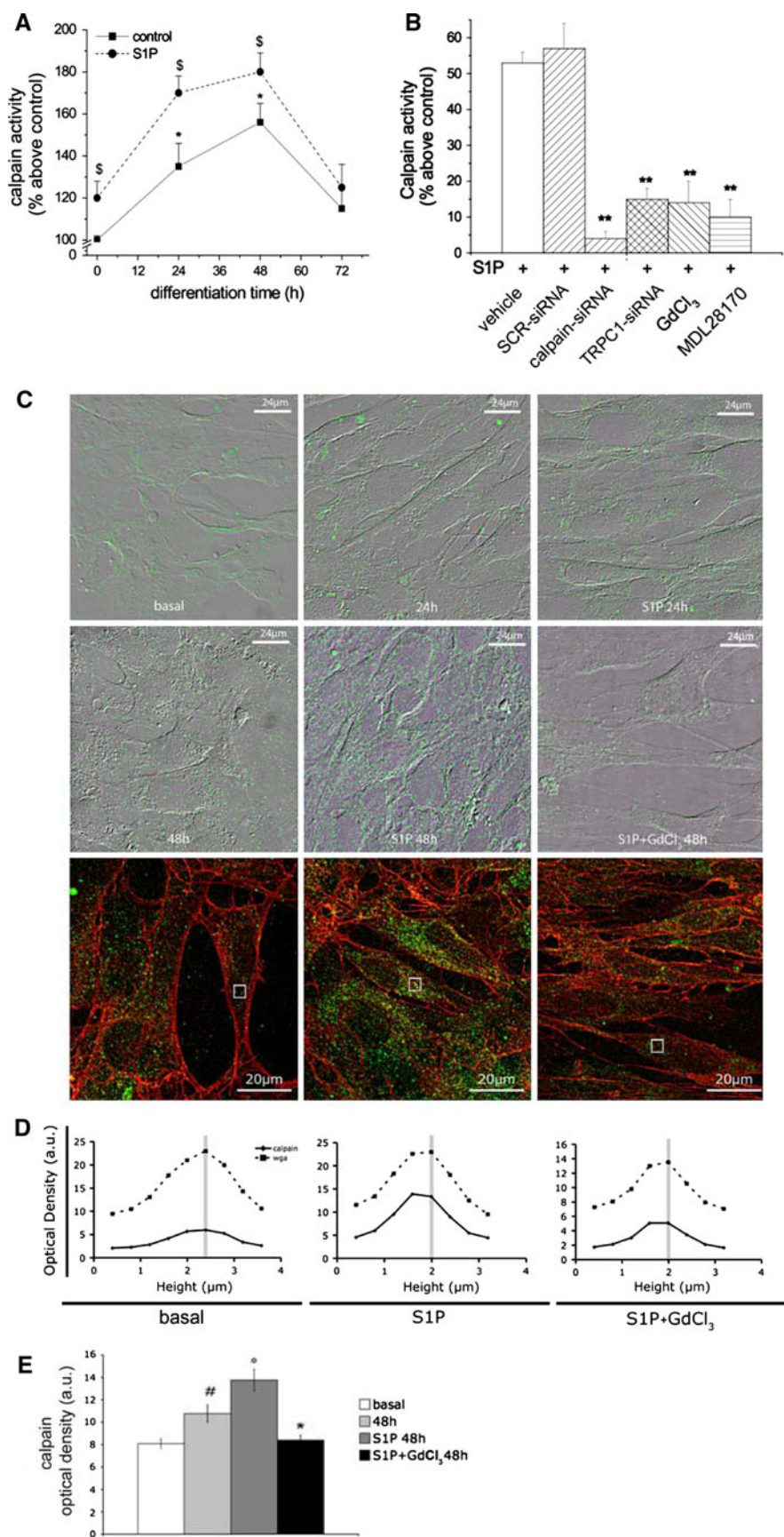
		A (mV ⁻¹)	V ₀ (mV)	G _{min}	G _{j,ss} (nS)
Control (24 h)	V _j (+)	0.061 ± 4 × 10 ⁻³	62.10 ± 4.4	0.25 ± 0.03	5.2 ± 0.5
	V _j (-)	0.072 ± 3 × 10 ⁻³ §	-51.11 ± 4.3§	0.45 ± 0.05§§	
SIP (24 h)	V _j (+)	0.061 ± 3 × 10 ⁻³	60.10 ± 5.2	0.33 ± 0.03*	26.1 ± 2.4++++
	V _j (-)	0.060 ± 3 × 10 ⁻³ *†	-55.09 ± 4.2§	0.32 ± 0.05**	
GdCl ₃ (24 h)	V _j (+)	0.050 ± 4 × 10 ⁻³ *	84.10 ± 4.3	0.29 ± 0.03*	2.6 ± 0.24+
	V _j (-)	0.052 ± 4 × 10 ⁻³ **	-44.09 ± 4.2§§*	0.35 ± 0.05§*	
GdCl ₃ + SIP (24 h)	V _j (+)	0.056 ± 4 × 10 ⁻³ †	80.10 ± 5.4	0.28 ± 0.03*	9.1 ± 0.9+
	V _j (-)	0.059 ± 5 × 10 ⁻³ *†	-45.09 ± 4.0§§*	0.38 ± 0.05§*	
TRPC1-siRNA (24 h)	V _j (+)	0.054 ± 4 × 10 ⁻³ *	75.10 ± 6.2**	0.30 ± 0.03*	3.1 ± 0.2+
	V _j (-)	0.055 ± 4 × 10 ⁻³ **	-48.09 ± 4.1§§	0.44 ± 0.04§§	
TRPC1-siRNA + SIP (24 h)	V _j (+)	0.059 ± 4 × 10 ⁻³ †	65.10 ± 5.2	0.30 ± 0.03*	14.3 ± 1.6++++
	V _j (-)	0.062 ± 4 × 10 ⁻³ **†	-55.09 ± 3.9§	0.32 ± 0.04**	
Control (48 h)	V _j (+)	0.075 ± 5 × 10 ⁻³ **	60.03 ± 5.7	0.27 ± 0.04	6.8 ± 0.7§
	V _j (-)	0.077 ± 4 × 10 ⁻³ *	-45.04 ± 4.2§§	0.25 ± 0.04**	
SIP (48 h)	V _j (+)	0.077 ± 4 × 10 ⁻³ **	59.04 ± 5.0	0.22 ± 0.06	33.8 ± 4.6++++\$\$
	V _j (-)	0.078 ± 5 × 10 ⁻³ *	-50.11 ± 4.5§	0.21 ± 0.05***	
GdCl ₃ (48 h)	V _j (+)	0.050 ± 5 × 10 ⁻³ *	66.11 ± 4.9	0.29 ± 0.04	2.0 ± 0.3+
	V _j (-)	0.048 ± 5 × 10 ⁻³ **	-47.11 ± 4.1§§	0.44 ± 0.04§§	
GdCl ₃ + SIP (48 h)	V _j (+)	0.053 ± 5 × 10 ⁻³ *	62.10 ± 5.7	0.26 ± 0.03	6.1 ± 0.4§
	V _j (-)	0.055 ± 4 × 10 ⁻³ **†	-54.12 ± 4.1§	0.45 ± 0.05§§	
TRPC1-siRNA (48 h)	V _j (+)	0.055 ± 5 × 10 ⁻³ *	65.11 ± 5.2	0.29 ± 0.04	3.0 ± 0.3+
	V _j (-)	0.052 ± 5 × 10 ⁻³ **	-48.11 ± 3.7§§	0.39 ± 0.04§*	
TRPC1-siRNA + SIP (48 h)	V _j (+)	0.056 ± 5 × 10 ⁻³ *	62.10 ± 6.2	0.24 ± 0.03	12.2 ± 1.5++++\$
	V _j (-)	0.056 ± 4 × 10 ⁻³ **	-52.12 ± 4.4§	0.38 ± 0.05§	

Physiological parameters were measured in SCR-siRNA (control), GdCl₃, and TRPC1-siRNA-treated myoblast pairs, in the absence or presence of SIP at 24 and 48 h of differentiation. Data were obtained by fitting normalized steady-state conductance (G_{j,ss}) versus voltage using Boltzmann function. G_{j,ss}, evaluated at 10 mV and expressed as absolute values, represents G_{max}. G_{min} values were normalized data respect to G_{max}. Statistical significance was calculated by one-way ANOVA: *p < 0.05 and **p < 0.01 respect to control at 24 h; §p < 0.05 and §§p < 0.01 represent V_j(-) versus V_j(+) respect to each cell pair; +p < 0.05, +++p < 0.01 and ++++p < 0.001 indicate G_{j,ss} values respect to 24 h control; \$p < 0.05 and \$\$p < 0.01 indicate G_{j,ss} at 48 h respect to 24 h; †p < 0.05 indicates A values in stimulated respect to SIP unstimulated. Data are mean ± SEM. For each experimental condition data were obtained from 22 to 27 cells. Data from SCR-siRNA-treated cells as well as from untreated (not shown) were not significantly different

differentiating myoblasts, especially in those stimulated with SIP for 48 h (Fig. 6a). Most importantly, the treatments with TRPC1-siRNA, calpain-siRNA (Fig. 6a), and 50 μM GdCl₃ (Fig. 6b), induced a significant up-regulation of the activated membrane-associated PKCα in SIP-stimulated cells (≈65%), implying a functional link between TRPC1 and the protein kinase isoform. The significant increase (≈120%) of overall Cx43 expression in membrane fractions of the cells treated with 5 μM Gö6976, a selective inhibitor of classical Ca²⁺-dependent PKCs, supported the involvement of these enzymes in the negative regulation of Cx43 protein in skeletal myoblasts (Fig. 7a). Moreover, by immunoprecipitation, the interaction between Cx43 and cortactin, a cortical actin binding protein previously shown to mediate Cx43 interaction at

the plasma membrane [6], was impaired by the inhibition of TRPC1/PKCα signaling in SIP-stimulated cells (Fig. 7b). In particular, the immunocomplex Cx43/cortactin was reduced of approximately of 55%, whereas Cx43 detected by Western blotting and confocal microscopy analyses was decreased in the presence of GdCl₃ of approximately of 80 and 70%, respectively. These latter findings suggest that GdCl₃ may affect the pool of Cx43 interacting with cortactin.

Given that phosphorylation of Cx43 by PKCα has been previously reported to affect the protein conformation and its interaction with other intracellular proteins [6, 22, 43–45], taken together all these data implied that TRPC1-mediated *m*-calpain/PKCα pathway was critically involved in Cx43 remodeling at the plasma membrane.



◀ **Fig. 4** *m*-Calpain activation and expression are affected by SIP and TRPC1 inhibition in differentiating C2C12 myoblasts. **a** Confluent C2C12 myoblasts were cultured in DM in the presence (*dashed line*) or absence (control; *continuous line*) of 1 μ M SIP for the indicated times. Calpain activity was determined in intact C2C12 cells using the membrane-permeable fluorescent peptide substrate Sue-LLVY-AMC as described in “Materials and methods”. Data are means \pm SEM of three independent experiments with similar results. Note that calpain activity increases at 24 and 48 h of differentiation and this increase is significantly enhanced by SIP ($*p < 0.05$ 24 h and 48 h versus T0 and $^{\circ}p < 0.05$ SIP-stimulated versus unstimulated (control) cells). **b** C2C12 cells were transfected with scrambled siRNA (SCR-siRNA), TRPC1-siRNA, *m*-calpain-siRNA or treated with vehicle (DMSO) or 50 μ M GdCl₃ and 30 μ M MDL28170 and cultured in DM in the presence of 1 μ M SIP for 48 h. Data are means \pm SEM of three independent experiments with similar results. $**p < 0.01$ treated versus controls. HEPES treatment was not significantly different from DMSO. Note that treatment with GdCl₃ and transfection with TRPC1-siRNA reduce SIP-induced calpain activity at a similar extent as treatment with MDL28170 and *m*-calpain-siRNA. **c** Superimposed DIC and confocal fluorescence images of C2C12 cells immunostained for *m*-calpain. Confluent C2C12 cells were grown on glass coverslips in proliferation medium (basal) and induced to differentiate by shifting in DM in the presence or absence of 1 μ M SIP for the indicated times. In some experiments, the cells were treated with 50 μ M GdCl₃ prior SIP stimulation. After fixation, the cells were stained with specific antibodies against calpain (*green*). **d** Confocal immunofluorescent analysis of plasma membrane localization of *m*-calpain. Living C2C12 cells on glass coverslips cultured in proliferation medium (basal) or in DM plus 1 μ M SIP in the presence or absence of 50 μ M GdCl₃ for 48 h, were incubated with TRITC-conjugated wheat germ agglutinin (WGA) to label plasma membrane (*red*) and then fixed and immunostained for calpain expression (*green*). *Yellow spots* in the representative confocal images indicate co-localization of *red* and *green* fluorescence signals. The images are representative of at least three separate experiments with similar results. The diagrams show the mean optical density of *m*-calpain (*continuous line*) and WGA (*dashed line*) fluorescent signals measured through the depth of 3D confocal stacks in the specific regions of interest indicated in the confocal images (*grey square*). The maximum of the *red fluorescence* value (WGA) corresponds to the focal plane of the membrane. Vertical *grey line* indicates the co-localization between the two signals. **e** Densitometric analysis of *m*-calpain fluorescence signal. Data are mean \pm SEM. $^{\#}p < 0.05$ 48 h versus basal, $^{\circ}p < 0.01$ SIP stimulated versus unstimulated and $*p < 0.05$ SIP + GdCl₃ versus SIP. Of note, SIP stimulates calpain expression and its plasma membrane redistribution within the first 48 h of differentiation and this response is prevented by GdCl₃.

Finally, the biological role played by the above reported signalling in skeletal myogenesis was confirmed by the experiments showing that the treatment with either GdCl₃, or TRPC1-siRNA or MDL28170 caused a robust reduction of the expression of myogenin, a key myogenic transcriptional factor, and of myotube formation in SIP-stimulated cells (Fig. 7c).

Discussion

In adult skeletal muscle fibers, intracellular increase of Ca²⁺ depends upon the activation of peculiar channels

which belong to the TRPC family, and function as store-dependent and mechanosensitive channels [4, 13, 34, 46]. Of interest, these channels have been recently implicated in the regulation of numerous physiological and pathological processes, such as skeletal muscle differentiation and Duchenne muscular dystrophy [4, 30, 46, 47]. An open question in the field of TRPC signaling is the identification of specific targets by which these Ca²⁺ gates can affect cell differentiation. In the present study, we contributed to shed some light on this issue, by showing that TRPC1 channel activity is required for the up-regulation of Cx43 expression elicited by SIP in skeletal myoblasts. The physiological significance of this interaction in skeletal myogenesis is consistent with the well-known role of Cx43 in synchronizing cell differentiation among contacting myoblasts [6, 25, 48], and in making them competent for syncytial fusion [6, 25, 49, 50]. In particular, we have shown that the functional link between TRPC1 and Cx43 protein in SIP-differentiating myoblasts involves the activation of *m*-calpain/classical PKCs axis, thus contributing to extend our knowledge on the molecular mechanisms by which SIP exerts its pro-myogenic action.

In perfect agreement with the postulated role for PKC α as a negative regulator of myogenesis, we showed here that the physiological decline of PKCs expression during myogenesis was associated with the up-regulation of Cx43 expression in SIP-differentiated myoblasts. These data gain support by the increasing evidence in the literature, showing the critical role played by phosphorylation events in the gap junction turnover [22, 29, 44]. In particular, several kinases, including PKC isoforms, casein kinase, mitogen-activated protein kinase (MAPK) and c-scr kinase, have been shown to phosphorylate the cytosolic carboxyl-terminal domain of Cx43 and mediate the protein internalization and degradation through the activation of lysosomal or proteosomal pathways [28, 29, 51, 52].

Interestingly, the here reported decrease in PKC α expression during C2C12 cell differentiation was prevented by *m*-calpain silencing and its specific inhibition, consistent with the accepted idea that this Ca²⁺-dependent kinase isoform is a good substrate for the cysteine protease [29, 33, 52]. Until now, the muscle-specific functions of calpains have been mainly restricted to the proteolysis of membrane and cytoskeletal proteins related to myoblast migration and fusion as well as to skeletal muscle dystrophy [31, 33, 35, 41, 53, 54]. Only recently, evidence exists for an involvement of these proteases in other aspects of myogenesis, including the regulation of myogenic transcriptional factors, such as MyoD, Myf5 and myogenin and phosphorylation of p38 MAPK [33, 55]. In such a view, the present data contribute to

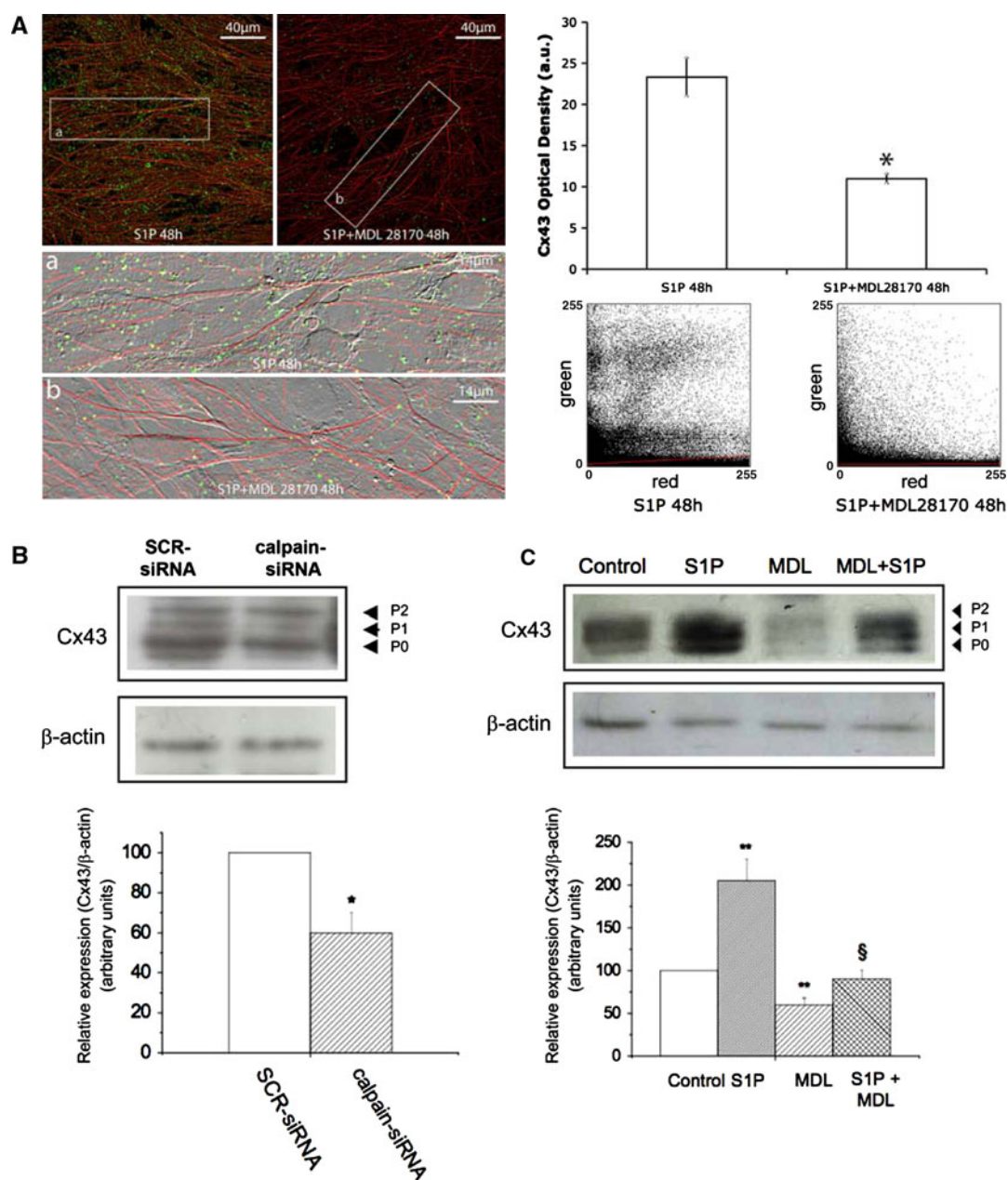


Fig. 5 *m*-Calpain is required for S1P-induced Cx43 expression in differentiating C2C12 myoblasts. **A** Confocal immunofluorescence images of confluent C2C12 cells cultured on glass coverslips in DM plus 1 µM S1P in the presence or absence of 30 µM MDL28170 for 48 h, fixed, immunostained for Cx43 expression (green), and counterstained with TRITC-phalloidin to reveal actin filaments (red). In the *histogram*, densitometric analysis of Cx43 fluorescent signal is reported. $*p < 0.05$. The images are representative of at least three separate experiments with similar results. **a, b** Superimposed DIC and fluorescence images of the selected insets showing colocalization of Cx43 with peripheral actin cytoskeleton. Scatterplots showing the distribution of sampled pixels plotted as a function of the green (y-axis, Cx43) and red (x-axis, stress fibers) emission intensity in the indicated experimental conditions. Colocalized pixels in the image are included along the diagonal axis. **B** C2C12 myoblasts were transfected with scrambled siRNA (SCR-siRNA) or calpain-siRNA, incubated in DM for 48 h and processed for Western-blot analysis.

Proteins (15 µg) obtained from membrane fractions were separated on SDS-PAGE and the content of Cx43 analyzed using specific anti-Cx43 antibodies. Band intensity, was reported as relative percentage of the ratio between overall Cx43/β-actin, normalized to control (SCR-siRNA), set as 100, as shown in the graphic. A blot representative of at least three independent experiments with similar results is shown. $*p < 0.05$. **C** C2C12 myoblasts were incubated in DM in the absence (control) or presence of 1 µM S1P and/or 30 µM MDL28170 (MDL) for 48 h and then processed for Western-blot analysis as in **B**. Band intensity was reported as relative percentage of the ratio between overall Cx43/β-actin, normalized to control, set as 100, as shown in the graphic. A blot representative of at least three independent experiments with similar results is shown. $**p < 0.01$ S1P and MDL versus control $§p < 0.05$ S1P + MDL versus S1P. Note that inhibition of calpain is accompanied by reduced Cx43 expression and localization along the peripheral stress fiber

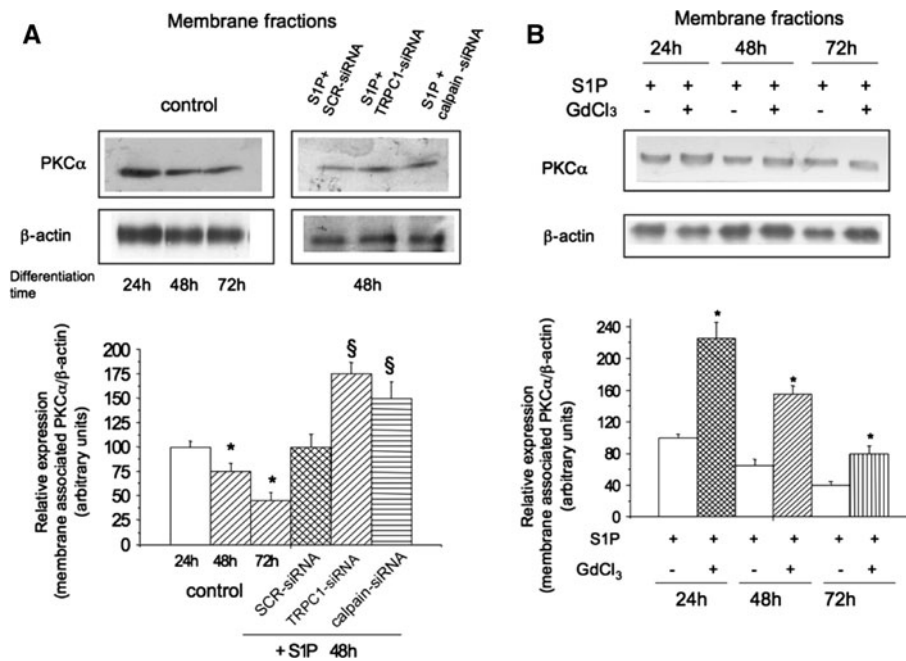


Fig. 6 TRPC1 inhibition prevents PKC α degradation in differentiating C2C12 myoblasts. **a** PKC α expression was determined in membrane fractions (25 μ g) obtained from C2C12 cells incubated in DM for the indicated times in the absence of 1 μ M S1P (control), centrifuged as described in “Materials and methods” and processed for Western blotting. In other experiments, C2C12 cells were transfected with scrambled siRNA (SCR-siRNA) or TRPC1-siRNA or *m*-calpain-siRNA and cultured in DM plus 1 μ M S1P for 48 h. Band intensity, reported as relative percentage of the ratio between overall PKC α / β -actin, to control (24 h or SCR-siRNA + S1P 48 h) arbitrarily normalized to 100 is shown in the graphic. Data (means \pm SEM) are representative of three independent experiments with similar results. * $p < 0.05$ 48 h and 72 h versus 24 h; $\S p < 0.05$

TRPC1-siRNA +S1P or *m*-calpain-siRNA + S1P versus SCR-siRNA + S1P. **b** PKC α expression was determined in membrane fractions (25 μ g) obtained from C2C12 cells incubated for the indicated times in DM plus 1 μ M S1P in the presence (+) or absence (-) of 50 μ M GdCl₃. Quantification of band intensity, shown in the graph, is reported as ratio of PKC α / β -actin, and relative to control normalized to 100. Data are representative of three independent experiments with similar results. * $p < 0.05$ S1P + GdCl₃ versus S1P. Note that the active pool of membrane associated-PKC α progressively decreases with myoblast differentiation both in unstimulated and S1P-stimulated cells and that the treatment with TRPC1-siRNA, *m*-calpain-siRNA and GdCl₃ prevents the reduction of active PKC α

extend the list of the biological actions of *m*-calpain in skeletal muscle, including Cx43 protein expression and membrane stability, as critical events of its action in the promotion of myogenesis by S1P. We may exclude a direct effect of calpain on Cx43, as reported on other connexin isoforms [56, 57], based on the findings that the genetic and pharmacological inhibition of the cysteine protease was associated with reduced, instead of increased, Cx43 expression levels in C2C12 myoblasts. Moreover, the cleavage of the C-terminal tail of the gap junction protein [27] by calpain may also be ruled out in our experimental conditions, considering that the protein detection in the Western-blot analysis was performed using specific antibodies against the C-terminal region of Cx43.

Of interest, we also demonstrated that *m*-calpain/classical PKC α axis and Cx43 up-regulation were dependent on the activation of TRPC1 channel by S1P during the early phases of differentiation, since reduced channel expression

and activity was able to dramatically affect *m*-calpain/PKC α pathway. By dual whole cell patch-clamp electrophysiological analysis, it was possible to reveal that TRPC1 functions were also required for the gap-junctional coupling and selectivity.

We finally tried to answer the question of how TRPC1/PKC α -dependent phosphorylation could affect Cx43 protein function in skeletal myoblasts. It has been previously reported by our group and others that actin-binding proteins provide a physical linkage between Cx43 and the cortical cytoskeleton and that these interactions are required for maintaining functional Cx43-formed gap junctions in differentiating myoblasts [6, 58]. Among the different proteins interacting with connexins are the ZO proteins, vinculin, ezrin, α -actin and cortactin [6, 47, 58]. In this study we showed that TRPC1 channels could regulate the remodeling of a specific pool of Cx43 protein, likely through the stabilization and coordination of its interaction with cortactin. This assumption is consistent

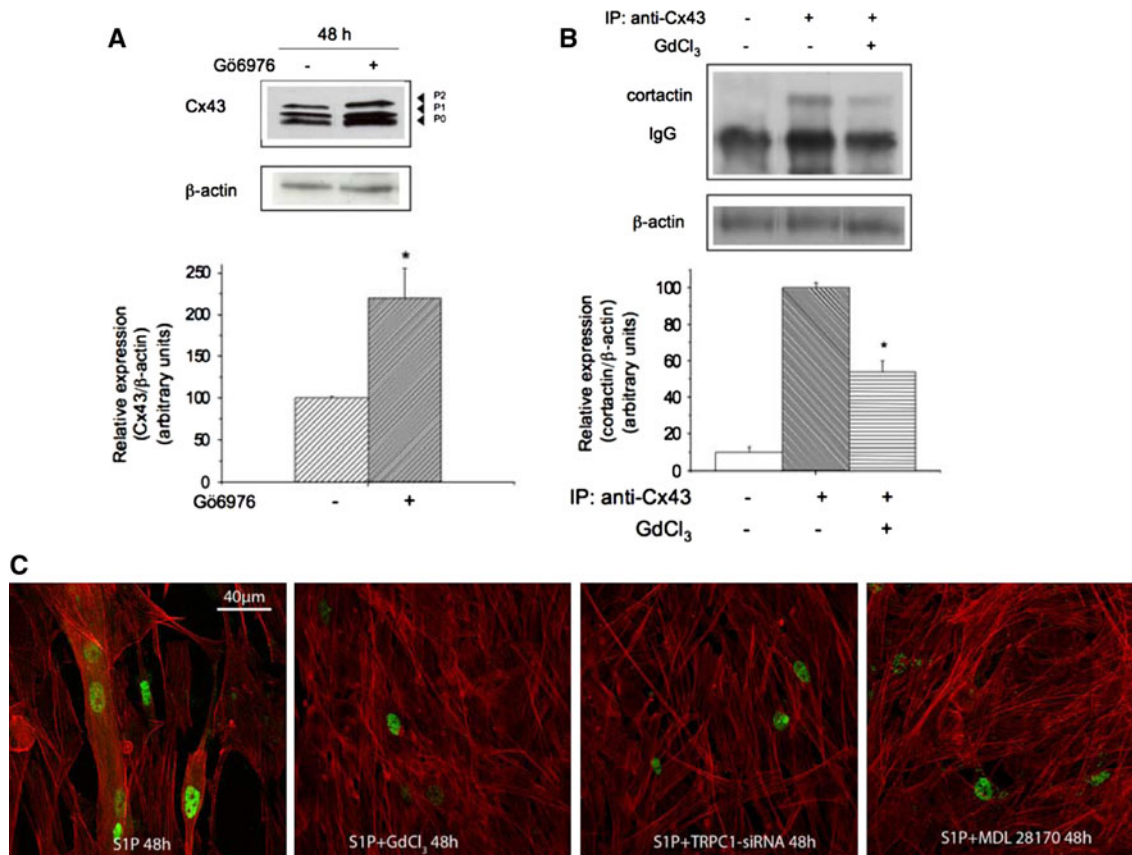


Fig. 7 TRPC1/calpain/PKC α axis is required for S1P-induced Cx43 expression, cortactin-Cx43 interaction and myoblast differentiation in C2C12 cells. **a** Western Blotting analysis of Cx43 expression. C2C12 cells were induced to differentiate in DM plus 1 μ M S1P in the presence (+) or absence (-) of 5 μ M Gö6976 for 48 h. Cx43 expression was immunodetected in membrane fractions (25 μ g) using specific polyclonal antibodies. A representative blot of three independent experiments is shown. Band intensity, reported as relative percentage normalized to control set as 100, is shown in the graphic. * $p < 0.05$. **b** Co-immunoprecipitation of Cx43 with cortactin. C2C12 cells were incubated in DM plus 1 μ M S1P in the presence (+) or absence (-) of 50 μ M GdCl₃ for 48 h. Immunoprecipitation with anti-Cx43 antibodies from cell lysates (+) was performed as reported in “Materials and methods”. The immuno-

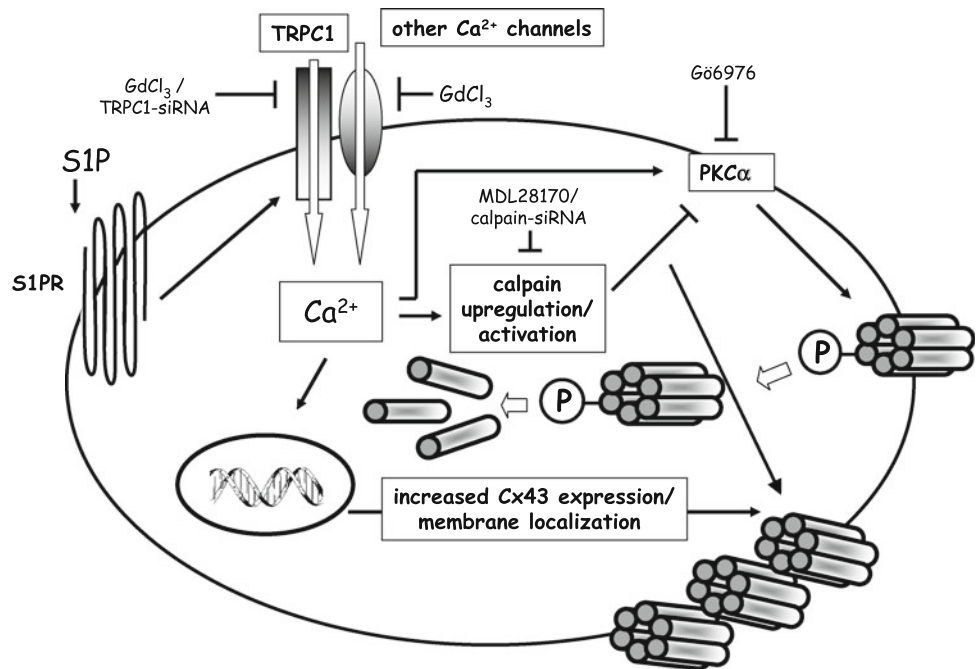
complexes were revealed with anti-cortactin antibodies. A blot representative of three independent experiments with similar results is reported. * $p < 0.05$ GdCl₃ versus control. Negative control (no primary antibodies) is shown. Note that S1P-induced Cx43–cortactin interaction requires TRPC1 activity in differentiating C2C12 myoblasts. **c** Confocal immunofluorescence images of confluent C2C12 cells cultured on glass coverslips in DM plus 1 μ M S1P for 48 h in the presence or absence of 50 μ M GdCl₃ and 30 μ M MDL28170, or transfected with TRPC1-siRNA fixed, immunostained for myogenin expression (green) and counterstained with TRITC-phalloidin to reveal actin filaments (red). The inhibition of GdCl₃-sensitive and TRPC1 channels as well as the treatment with the calpain inhibitor results in a marked reduction of myogenin-positive nuclei and myotube formation

with previous observations in the literature showing that Ca²⁺/ PKC α -dependent phosphorylation of connexins [44] can influence their interaction with other proteins at the plasma membrane [22, 45].

In conclusion, taken together, the present findings show for the first time that TRPC1 channels are involved in Cx43 protein expression in skeletal myoblasts stimulated to differentiate by S1P, and propose that the key events downstream the activation of the Ca²⁺ channels, are represented by *m*-calpain activation, calpain-dependent PKC α reduction and Cx43 protein plasma membrane stabilization

(see diagram Fig. 8). The identification of this pathway may contribute to increase our knowledge on the role played by S1P and TRPC1-mediated Ca²⁺ signaling in skeletal myogenesis, involving the expression of proteins with short half-life turnover, such as connexins, whose regulation is essential for many cellular functions [24, 59, 60]. In our opinion, the newly identified pathway may represent a stimulus for the development of selective pharmacological compounds with possible applications in the treatment of skeletal muscle disorders characterized by impaired TRPC channel function.

Fig. 8 Molecular mechanisms underlying the effects of S1P on Cx43 expression, membrane association, and stabilization. The activation of S1P-specific receptors induces TRPC1 and $GdCl_3$ -sensitive channel opening and, in turn, promotes Ca^{2+} entry, followed by the activation of *m*-calpain, a calcium-dependent protease. This causes a decrease in PKC α activity, due to proteolysis, and, as a consequence, a decrease of Cx43 phosphorylation and internalization. Together with enhanced Cx43 biosynthesis induced by elevated intracellular Ca^{2+} , this results in increased amount of Cx43 in cell membranes following S1P stimulation



Acknowledgments This work was supported by grants from Fondazione Cassa di Risparmio di Pistoia e Pescia to E.M., Fondazione Banche di Pistoia e Vignole to E.M., Ente Cassa di Risparmio di Firenze to L.F., S.Z.-O., Programma Vigoni to E.M., and from the Italian Ministry for Education, University and Research, Rome, Italy to E.M., L.F., C.S., F.F. and S.Z.-O. The authors are grateful to Dr. Daniele Nosi (Dept. of Anatomy, Histology and Forensic Medicine, University of Florence, Florence, Italy) for his valuable contribution in confocal image acquisition and processing.

References

- Kim RH, Takabe K, Milstien S, Spiegel S (2009) Export and functions of sphingosine-1-phosphate. *Biochim Biophys Acta* 179:692–696
- Nagata Y, Kobayashi H, Umeda M, Ohta N, Kawashima S, Zammit PS, Matsuda R (2006) Sphingomyelin levels in the plasma membrane correlate with the activation state of muscle satellite cells. *J Histochem Cytochem* 54:375–384
- Nagata Y, Partridge TA, Matsuda R, Zammit PS (2006) Entry of muscle satellite cells into the cell cycle requires sphingolipid signaling. *J Cell Biol* 174:245–253
- Formigli L, Sassoli C, Squecco R, Bini F, Martinesi M, Chellini F, Luciani G, Sbrana F, Zecchi-Orlandini S, Francini F, Meacci E (2009) Regulation of transient receptor potential canonical channel 1 (TRPC1) by sphingosine 1-phosphate in C2C12 myoblasts and its relevance for a role of mechanotransduction in skeletal muscle differentiation. *J Cell Sci* 122:1322–1333
- Meacci E, Nuti F, Donati C, Concetti F, Farnararo M, Bruni P (2008) Sphingosine kinase activity is required for myogenic differentiation of C2C12 myoblasts. *J Cell Physiol* 214:210–220
- Squecco R, Sassoli C, Nuti F, Nosi D, Chellini F, Zecchi-Orlandini S, Francini F, Formigli L, Meacci E (2006) Sphingosine 1-phosphate induces myoblast differentiation through Cx43 protein expression: role for a gap junction-dependent and -independent function. *Mol Biol Cell* 17:4896–4910
- Zanin M, Germinario E, Dalla Libera L, Sandonà D, Sabbadini RA, Betto R, Danieli-Betto D (2008) Trophic action of sphingosine 1-phosphate in denervated rat soleus muscle. *Am J Physiol Cell Physiol* 294:C36–C46
- Formigli L, Francini F, Meacci E, Vassalli M, Nosi D, Quercioli F, Tiribilli B, Bencini C, Piperio C, Bruni P, Orlandini SZ (2002) Sphingosine 1-phosphate induces Ca^{2+} transients and cytoskeletal rearrangement in C2C12 myoblastic cells. *Am J Physiol Cell Physiol* 282:C1361–C1373
- Meacci E, Cencetti F, Formigli L, Squecco R, Donati C, Tiribilli B, Quercioli F, Zecchi Orlandini S, Francini F, Bruni P (2002) Sphingosine 1-phosphate evokes calcium signals in C2C12 myoblasts via Edg3 and Edg5 receptors. *Biochem J* 362:349–357
- Abramowitz J, Birnbaumer L (2009) Physiology and pathophysiology of canonical transient receptor potential channels. *FASEB J* 23:297–328
- Formigli L, Meacci E, Sassoli C, Squecco R, Nosi D, Chellini F, Naro F, Francini F, Zecchi-Orlandini S (2007) Actin cytoskeleton/stretch-activated ion channels interaction regulates myogenic differentiation of skeletal myoblasts. *J Cell Physiol* 211:296–306
- Formigli L, Meacci E, Sassoli C, Chellini F, Quercioli F, Tiribilli B, Squecco R, Bruni P, Francini F, Zecchi-Orlandini S (2005) Sphingosine 1-phosphate induces cytoskeletal reorganization in C2C12 myoblasts: physiological relevance for stress fibres in the modulation of ion current through stretch-activated channels. *J Cell Sci* 118:1161–1171
- Sbrana F, Sassoli C, Meacci E, Nosi D, Squecco R, Paternostro F, Tiribilli B, Zecchi-Orlandini S, Francini F, Formigli L (2008) Role for stress fiber contraction in surface tension development and stretch-activated channel regulation in C2C12 myoblasts. *Am J Physiol Cell Physiol* 295:C160–C172
- Su Z, Zhou X, Loukin SH, Haynes WJ, Saimi Y, Kung C (2009) The use of yeast to understand TRP-channel mechanosensitivity. *Pflugers Arch* 458:861–867
- Stauf S, Maxvill I, Lind U, Husmark J, Mattsson J, Ernfors P, Pierrou S (2009) Down regulation of TRPC1 by shRNA reduces mechanosensitivity in mouse dorsal root ganglion neurons in vitro. *Neurosci Lett* 457:3–7

16. Sharif-Naeini R, Dedman A, Folgering JH, Duprat F, Patel A, Nilius B, Honoré E (2008) TRP channels and mechanosensory transduction: insights into the arterial myogenic response. *Pflügers Arch* 456:529–540
17. Folgering JH, Sharif-Naeini R, Dedman A, Patel A, Delmas P, Honoré E (2008) Molecular basis of the mammalian pressure-sensitive ion channels: focus on vascular mechanotransduction. *Prog Biophys Mol Biol* 97:180–195
18. Zanou N, Shapovalov G, Louis M, Tajeddine N, Gallo C, Van Schoor M, Anguish I, Cao ML, Schakman O, Dietrich A, Lebacqz J, Rugg U, Roulet E, Birnbaumer L, Gailly P (2010) Role of TRPC1 channel in skeletal muscle function. *Am J Physiol Cell Physiol* 298:C149–C162
19. Ambudkar IS, Ong HL, Liu X, Bandyopadhyay BC, Cheng KT (2007) TRPC1: the link between functionally distinct store-operated calcium channels. *Cell Calcium* 42:213–223
20. Rodríguez-Sinovas A, Cabestrero A, López D, Torre I, Morente M, Abellán A, Miró E, Ruiz-Meana M, García-Dorado D (2009) The modulatory effects of connexin 43 on cell death/survival beyond cell coupling. *Prog Biophys Mol Biol* 94:219–232
21. Söhl G, Willecke K (2004) Gap junctions and the connexin protein family. *Cardiovasc Res* 62:228–232
22. Solan JL, Lampe PD (2009) Connexin 43 phosphorylation: structural changes and biological effects. *Biochem J* 15:261–272
23. Araya R, Eckardt D, Maxeiner S, Kruger O, Theis M, Willecke K, Saez JC (2005) Expression of connexins during differentiation and regeneration of skeletal muscle: functional relevance of connexin 43. *J Cell Sci* 118:27–37
24. Dobrowolski R, Willecke K (2009) Connexin-caused genetic diseases and corresponding mouse models. *Antioxid Redox Signal* 11:283–295
25. Cruciani V, Mikalsen SO (2006) The vertebrate connexin family. *Cell Mol Life Sci* 63:1125–1140
26. Butkevich E, Hulsman S, Wenzel D, Shiraro T, Duden R, Majoul I (2004) Drebrin is a novel connexin-43 binding partner that links gap junctions to the submembrane cytoskeleton. *Curr Biol* 14:650–658
27. Joshi-Mukherjee R, Coombs W, Burrer C, Alvarez de Mora I, Delmar M, Taffet S (2007) Evidence for the presence of a free C-terminal fragment of Cx43 in cultured cells. *Cell Commun Adhes* 14:75–84
28. Hervé JC, Plaisance I, Loncarek J, Duthe F, Sarrouilhe D (2004) Is the junctional uncoupling elicited in rat ventricular myocytes by some dephosphorylation treatments due to changes in the phosphorylation status of Cx43? *Eur Biophys J* 33:201–210
29. Laird DW (2005) Connexin phosphorylation as a regulatory event linked to gap junction internalization and degradation. *Biochim Biophys Acta* 1711:172–182
30. Grossi A, Karlsson AH, Lawson MA (2008) Mechanical stimulation of C2C12 cells increases *m*-calpain expression, focal adhesion plaque protein degradation. *Cell Biol Int* 32:615–622
31. Honda M, Masui F, Kanzawa N, Tsuchiya T, Toyo-oka T (2008) Specific knockdown of *m*-calpain blocks myogenesis with cDNA deduced from the corresponding RNAi. *Am J Physiol Cell Physiol* 294:C957–C965
32. Kramerova I, Kudryashova E, Wu B, Spencer MJ (2006) Regulation of the M-cadherin-beta-catenin complex by calpain 3 during terminal stages of myogenic differentiation. *Mol Cell Biol* 26:8437–8447
33. Liang YC, Yeh JY, Forsberg NE, Ou BR (2006) Involvement of μ - and *m*-calpains and protein kinase C isoforms in L8 myoblast differentiation. *Int J Biochem Cell Biol* 38:662–670
34. Ducret T, Vandebrouck C, Cao ML, Lebacqz J, Gailly P (2006) Functional role of store-operated and stretch-activated channels in murine adult skeletal muscle fibers. *J Physiol* 575:913–924
35. Raynaud F, Carnac G, Marcilhac A, Benyamin Y (2004) *m*-Calpain implication in cell cycle during muscle precursor cell activation. *Exp Cell Res* 298:48–57
36. Meacci E, Donati C, Cencetti F, Romiti E, Bruni P (2000) Permissive role of protein kinase C alpha but not protein kinase C delta in sphingosine 1-phosphate-induced Rho A activation in C2C12 myoblasts. *FEBS Lett* 482:97–101
37. Meacci E, Cencetti F, Donati C, Nuti F, Farnararo M, Kohno T, Igarashi Y, Bruni P (2003) Down-regulation of EDG5/S1P2 during myogenic differentiation results in the specific uncoupling of sphingosine 1-phosphate signalling to phospholipase D. *Biochim Biophys Acta* 1633:133–142
38. Meacci E, Donati C, Cencetti F, Oka T, Komuro I, Farnararo M, Bruni P (2001) Dual regulation of sphingosine 1-phosphate-induced phospholipase D activity through RhoA and protein kinase C-alpha in C2C12 myoblasts. *Cell Signal* 13:593–598
39. Sasaki T, Kikuchi T, Yumoto N, Yoshimura N, Murachi T (1984) Comparative specificity and kinetic studies on porcine calpain I and calpain II with naturally occurring peptides and synthetic fluorogenic substrates. *J Biol Chem* 259:12489–12494
40. Lampe PD, Cooper CD, King TJ, Burt JM (2006) Analysis of Connexin43 phosphorylated at S325, S328 and S330 in normoxic and ischemic heart. *J Cell Sci* 119:3435–3442
41. Louis M, Zanou N, Van Schoor M, Gailly P (2008) TRPC1 regulates skeletal myoblast migration and differentiation. *J Cell Sci* 121:3951–3959
42. Williams AB, Decourten-Myers GM, Fischer JE, Luo G, Sun X, Hasselgren PO (1999) Sepsis stimulates release of myofilaments in skeletal muscle by a calcium-dependent mechanism. *FASEB J* 13:1435–1443
43. Buday L, Downward J (2007) Roles of cortactin in tumor pathogenesis. *Biochim Biophys Acta* 1775:263–273
44. Sirnes S, Kjenseth A, Leithe E, Rivedal E (2009) Interplay between PKC and the MAP kinase pathway in Connexin43 phosphorylation and inhibition of gap junction intercellular communication. *Biochem Biophys Res Commun* 382:41–45
45. Sosinsky GE, Solan JL, Gaietta GM, Ngan L, Lee GJ, Mackey MR, Lampe PD (2007) The C-terminus of connexin43 adopts different conformations in the Golgi and gap junction as detected with structure-specific antibodies. *Biochem J* 408:375–385
46. Vandebrouck A, Sabourin J, Rivet J, Balghi H, Sebille S, Kitzis A, Raymond G, Cognard C, Bourmeyster N, Constantin B (2007) Regulation of capacitative calcium entries by 1-syntrophin: association of TRPC1 with dystrophin complex and the PDZ domain of 1-syntrophin. *FASEB J* 21:608–617
47. Stiber J, Hawkins A, Zhang ZS, Wang S, Burch J, Graham V, Ward CC, Seth M, Finch E, Malouf N, Williams RS, Eu JP, Rosenberg P (2008) STIM1 signaling controls store-operated calcium entry required for development and contractile function in skeletal muscle. *Nat Cell Biol* 10:688–697
48. Trovato-Salinaro A, Belluardo N, Frinchi M, von Maltzahn J, Willecke K, Condorelli DF, Mudò G (2009) Regulation of connexin gene expression during skeletal muscle regeneration in the adult rat. *Am J Physiol Cell Physiol* 296:C593–C606
49. Kalderon N, Epstein ML, Gilula NB (1977) Cell-to-cell communication and myogenesis. *J Cell Biol* 75:788–806
50. von Maltzahn J, Wulf V, Willecke K (2006) Spatiotemporal expression of connexin 39 and -43 during myoblast differentiation in cultured cells and in the mouse embryo. *Cell Commun Adhes* 13:55–60
51. Hervé JC, Derangeon M, Bahbouhi B, Mesnil M, Sarrouilhe D (2007) The connexin turnover, an important modulating factor of the level of cell-to-cell junctional communication: comparison with other integral membrane proteins. *J Membr Biol* 217:21–33
52. Rivedal E, Leithe E (2005) Connexin43 synthesis, phosphorylation, and degradation in regulation of transient inhibition of gap

- junction intercellular communication by the phorbol ester TPA in rat liver epithelial cells. *Exp Cell Res* 302:143–152
53. Bertipaglia I, Carafoli E (2007) Calpains and human disease. *Subcell Biochem* 45:29–53
54. Goel HL, Dey CS (2002) PKC-regulated myogenesis is associated with increased tyrosine phosphorylation of FAK, Cas, and paxillin, formation of Cas-CRK complex, and JNK activation. *Differentiation* 70:257–271
55. Kook SH, Choi KC, Son YO, Lee KY, Hwang IH, Lee HJ, Chung WT, Lee CB, Park JS, Lee JC (2008) Involvement of p38 MAPK-mediated signaling in the calpeptin-mediated suppression of myogenic differentiation and fusion in C2C12 cells. *Mol Cell Biochem* 310:85–92
56. Lin JS, Fitzgerald S, Dong Y, Knight C, Donaldson P, Kistler J (1997) Processing of the gap junction protein connexin50 in the ocular lens is accomplished by calpain. *Eur J Cell Biol* 73:141–149
57. Zhang W, Ma X, Zhong M, Zheng Z, Li L, Wang Z, Zhang Y (2009) Role of the calpain system in pulmonary vein connexin remodeling in dogs with atrial fibrillation. *Cardiology* 112:22–30
58. Vitale ML, Akpovi CD, Pelletier RM (2009) Cortactin/tyrosine-phosphorylated cortactin interaction with connexin 43 in mouse seminiferous tubules. *Microsc Res Tech* 72:856–867
59. Kardami E, Dang X, Iacobas DA, Nickel BE, Jeyaraman M, Srisakuldee W, Makazan J, Tanguy S, Spray DC (2007) The role of connexins in controlling cell growth and gene expression. *Prog Biophys Mol Biol* 94:245–264
60. Park JH, Lee MY, Heo JS, Han HJ (2008) A potential role of connexin 43 in epidermal growth factor-induced proliferation of mouse embryonic stem cells: involvement of Ca^{2+} /PKC, p44/42 and p38 MAPKs pathways. *Cell Prolif* 41:786–802